42nd European Photovoltaic Solar Energy Conference and Exhibition

This presentation was selected by the Sc. Committee of the EU PVSEC 2025 for submission of a full paper to one of the EU PVSEC's collaborating peer-reviewed journals.

ASYNCHRONOUS DAYLIGHT LUMINESCENCE OBTAINED WITHOUT PROGRAMMABLE POWER SOURCES

Cristian Terrados[1,2], Eva de la Viuda[1], Kabir Paul Sulca[1], Julian Anaya[1], Miguel Ángel González[1], Oscar Martínez[1*]
(1) GdS-Optronlab group, Dpto. Física de la Materia Condensada. Universidad de Valladolid. Edificio LUCIA. Paseo de Belén, 11. Valladolid (Spain)
(2) Solar and Wind Feasibility Technologies (SWIFT). Escuela Politécnica Superior, Universidad de Burgos. Avda. Cantabria s/n 09006 Burgos (Spain)
*oscar.martinez@uva.es

ABSTRACT: Daylight Electroluminescence and Photoluminescence techniques (dEL/dPL) have rapidly advanced in recent years and are now well-established tools for the characterization of photovoltaic (PV) Si solar modules in the field. Performing dEL/dPL requires cameras capable of working in the near IR region of the light spectrum (such as InGaAs cameras) and sophisticated filtering procedures to distinguish the weak luminescence emission coming from the PV module from the more intense ambient light. Effective filtering of the weak luminescence requires specific acquisition schemes, both synchronous and asynchronous methods can be used for this purpose. Asynchronous schemes are more convenient, but they usually rely in expensive programmable power sources that produce high quality square or sinusoidal waveforms for the controlled current injection into the PV modules. When paired with fast InGaAs cameras (600 fps), dEL images can be obtained using very short (sub-second) acquisition times. However, the requirement for these programmable power sources may be a significant barrier to rapid in-field deployment of the technique. In this work we show the results of using asynchronous daylight luminescence inspections obtained without programmable power sources, using external control to modulate a DC signal from any power source, including the neighbor panels, or even without the use of a power source but using the Sun as the light source, in the dPL case. We specifically study the shape of the generated current and voltage signals, comparing the external control case with the case of using a programable power source. We also study the impact of varying the modulation frequency and camera speed on image quality and how these acquisition parameters influence performance. This approach broadens the applicability of the dEL technique, enabling effective filtering and identification of panel defects under self-powered or sunlight-driven conditions.
Keywords: daylight luminescence, module inspection, signal modulation, electroluminescence, photoluminescence

1 INTRODUCTION

Luminescence imaging techniques (EL/PL) are very well-established techniques for inspecting the condition of Si PV panels, providing complementary, and often more comprehensive information, compared to infrared thermography (IRT) and I-V characterization techniques [1, 2]. Given the large number of solar modules in a PV plant, the industry increasingly demands fast inspection techniques. For this reason, it is highly beneficial to perform on-site inspections at the solar plant without disassembling the modules, and preferably during the day. This allows for a rapid inspection of the modules and reduces the risk of damage during assembly and disassembly [3, 4]. In this context, daylight imaging techniques, such as dEL and dPL, have recently emerged and advanced rapidly [5-12]. However, it is still challenging to deploy these techniques effectively in a PV plant with a large number of modules. In this work we show a procedure that holds the potential to enable massive inspection of Si solar plants using these powerful techniques. For characterization we use the asynchronous mode, in which a modulated "on" and "off" signal allows for the filtration of the ambient light and allows to obtain the luminescence coming from the PV panels [13, 14]. In our asynchronous approach [14], we have previously used a large (15 kW) programable power source allowing for the high-quality modulated injection of current for a whole solar PV string. In the present work, we use instead an external and compact device to modulate the signal that can arise from any power source, including small and large DC power sources, but also the neighbor panels (self-powering configuration [15]), or even without the use of a power source but using the Sun as the light source, in the dPL case [9, 10, 16]. Combining fast InGaAs cameras, with maximum acquisition speeds of up to 600 fps, adequate optical filters to block as much ambient light as possible, and advanced filtering of the acquired light, allows dEL/dPL images to be recorded in very short times. This process, which eliminates the need for high-quality external programmable power sources to be connected to each string, has therefore the potential to provide a fast and cost-effective inspection of solar modules condition – a growing necessity for the operation and maintenance of medium-to-large solar plants.

To make a comparison with the case of using programmable power sources, we examine the shape of the generated current and voltage signals, as well as the quality of the final dEL image, for modulated signals obtained using a programable power source or those obtained by means of our external control device. We also examine how varying the modulation frequency and camera speed impacts image quality and the effect of these acquisition parameters on performance.

2 EXPERIMENTAL DETAILS

2.1 External device for signal modulation

A compact external device (ED) for square-wave signal modulation has been designed by means of an Arduino-based switching device, incorporating an XBee module for wireless control. The time periods of the "on" and "off" domains are defined and communicated remotely to an IGBT capable of switching up to 1500 V and 15 A. In this way, by connecting the ED to a DC power supply, current is injected into a PV module or string in a square wave scheme, where the frequency of the wave can

10.4229/EUPVSEC2025/3BO.11.5
020205-001

be easily adjusted. For instance, we have tested frequencies values of 6.25, 12.5, 25.0 and 50.0 Hz. One important advantage of this method is that square-wave signal modulation is generated independently of the power source, including the self-powering configuration of a PV string [15], and can be also applied for the dPL configuration, without the use of a power source, but just using the Sun for excitation and modifying (modulating) the position on the I-V curve to obtain two points with a large difference in currents drawn from the modules [16]. In this way, we can generate square "on" and "off" signals from any power source, also for the dPL case, eliminating the need for expensive, programmable power supplies, and simplifying in-field deployment of the dEL/dPL techniques.

2.1 Asynchronous scheme and experimental set-up

The acquisition of the dEL/dPL images is performed in an asynchronous scheme with the use of a high-speed camera, First Ligh C-RED 2 Lite, 640x512 – ~0.33 Mpixel – and pixel pitch of 15 x 15 µm, with 14-bit quantization and 16-bit dynamical range, with maximum speed of 600 fps. For these measurements, we have used 200 and 400 fps for the InGaAs camera speed. We have fixed the exposition time to 2.5 ms for all the measurements. We use a Kowa short wave infrared (SWIR) optical system with 16 mm focal length for image acquisition. A SWIR bandpass filter, centered around 1160 nm with a bandwidth of 150 nm and a transmittance close to 90%, is used in order to suppress as much ambient light as possible.

Multi-crystalline Si Al-BSF modules (Sharp, ND-AR330H 330 W, V_{oc}=45.5 V, I_{sc}=9.40 A) were used for the dEL/dPL tests. For the dEL case, we performed the signal modulation for just one module, using both a small power source (600 W, labelled as SPS) and the ED, as well as a large programmable power source (EA-PS 91500-30 3U 19" 3U 15000W model, labelled LPPS), which allows us to compare the signal modulation obtained from the programmable power source itself with the one obtained with the ED acting on a DC signal from this LPPS. We also performed dEL measurements exciting a string of 8 modules, also comparing the signal modulation obtained from the LPPS itself with the one obtained with the use of the ED acting on a DC signal from the LPPS. In both cases the injected current was fixed to the I_{sc} value of the modules. We also performed dEL measurements in the self-powering configuration [15], with two modules powering the inspected one, using the ED for signal modulation. We have also performed dPL measurements, using the Sun as the excitation source [10, 16] (that without the need of a power source), using also the ED for signal modulation. In all cases we have recorded both the current intensity and voltage waveforms at the entrance of one inspected module, using Fluke 80i-110s and Fluke 80K-40 probes, respectively.

The obtained whole stack of images is subsequently analyzed in the frequency domain using robust methods previously described [14] to obtain the final luminescence image from the PV panels. The quality of these images can be influenced by the noise and characteristics of the modulated signals. Therefore, the final images are thoroughly analyzed for various acquisition parameters using our previously proposed SNR_{25} metric [14].

3 RESULTS

3.1 dEL inspection of one module by acting on the SPS

The use of non-programmable DC power sources for injecting current into the modules is the standard procedure for EL image inspections on the dark. In particular, the EL inspection of just one Si module can be performed by a small DC power source, able to inject a current close to their I_{sc} value. On the other hand, for the case of dEL inspections, a signal modulation is needed. In this case, an external device to produce the signal modulation is thus required. We have already used in the past our developed ED for signal modulation of a DC signal, but in the synchronous mode, where the signal frequency is highly coupled to the camera speed [10, 16]. Here we have performed the dEL inspection of just one module by acting on a SPS, but in the asynchronous configuration, using different cameras velocities and signal frequencies, which in this case are decoupled.

Fig.1 (a, d) shows the measured current intensities and voltages at the entrance of the inspected module, reflecting the signal modulation performed by means of the ED acting on the SPS. The figure shows the case of two frequencies (25.0 Hz and 50.0 Hz). It can be observed that a non-perfect square wave form was obtained, with transients at the beginning of the "on" periods, with a duration of approx. 8-9 ms, independently of the used frequency. The figure also shows the pixel intensity captured by the InGaAs camera vs the number of images, for camera´s acquisition velocities of 200 and 400 fps for each frequency.

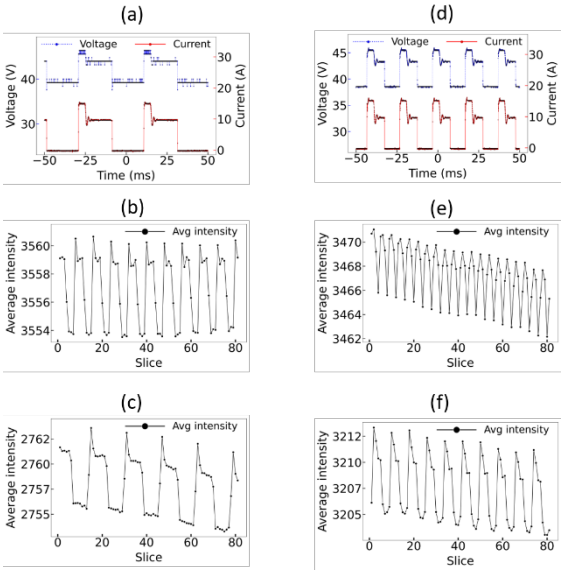

Figure 1: (a, d) Current intensities and voltages at the entrance of the inspected module, generated with the ED acting on a SPS, for ν=25.0 Hz (a) and ν=50.0 Hz (d). (b-f) Pixel intensity variations measured with the InGaAs camera vs number of images, corresponding to situation (a) (ν=25.0 Hz) for cameras´ velocities of 200 fps (b) and 400 fps (c), and to situation (d) (ν=50 Hz) for cameras´ velocities of 200 fps (e) and 400 fps (f), respectively

Thus, the use of the ED acting on the SPS for signal modulation produces a significative transient in both current intensity and voltage signals, with a large extension in time and a significative increase in the current

10.4229/EUPVSEC2025/3BO.11.5
020205-002

intensity values at the beginning of each cycle. Moreover, the transient in the signal modulation is clearly reflected in the measured pixel intensity. The final dEL images obtained applying the post-processing procedure to different sub-stacks of images are shown in Fig. 2 for frequencies of 12.5 and 25.0 Hz, and a camera speed of 400 fps (G=830 W/m^2). The obtained SNR_{25} marker is good enough (see the following comments), for the case of processing 400 images (Fig. (2b, d)), although the images have some minor errors for the case ν=12.5 Hz. Incorrect processing (with many errors) is observed for the case of processing a lower number of images for a frequency of 12.5 Hz (Fig. 2a); on the other hand, a good image quality is observed for a frequency of 25.0 Hz even processing only a sub-stack of 100 images (Fig. 2c).

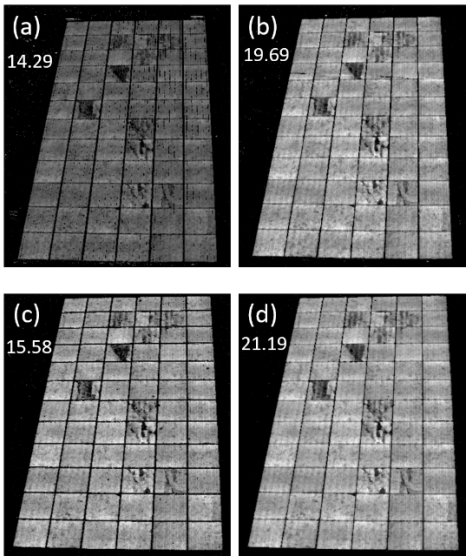

Figure 2: dEL images obtained after post-processing different sub-stacks of images, corresponding to the case of using a SPS, using the ED for square signal modulation. (a, b) ν=12.5 Hz, camera speed 400 fps; (a: post-processing of the first 250 images, b: post-processing of the whole 400 images of the stack). (c, d) ν=25.0 Hz, camera speed 400 fps; (c: post-processing of the first 100 images, d: post-processing of the whole 400 images of the stack) (in all cases G=830 W/m^2) (The SNR_{25} value is indicated on the right upper part of the images)

In this way, the transients do not seem to have a significant impact on the final quality of the dEL images. However, it would be preferable to avoid this type of transients, in order to prevent any effect on the power supply itself.

3.2 dEL inspection of one module by acting on the LPPS

The use of the LPPS allows us to directly compare the signal modulation produced by the power source itself with the modulation produced by means of our ED acting on a DC signal from the LPPS; in this section we show the case of exciting just only one module. Figure 3 shows the current intensities and voltages measured at the entrance of the module for both situations (for ν=50.0 Hz). It can be observed that the LPPS itself produces a perfect square signal (Fig. 3a). On the other hand, the ED acting on the LPPS (DC signal) produces a quite good square signal, except for the introduction, again, of a transient at the beginning of the cycles (Fig. 3d). This transient is now very sharp, with an insignificant time duration; however, there is a large increase in current intensity. Fig. 3 (b-f) also shows the pixel intensity variations vs number of images measured with the InGaAs camera, at speeds of 200 and 400 fps. It can be observed now that the transient in current intensities produced by the ED is not reflected in the pixel intensities (Fig. 3(e, f)), which is ascribed to the very fast transient. In this case, the post-processing of the stack of images is completely similar for both situations. For instance, Figure 4 shows the obtained dEL images after processing a sub-stack of 200 images for a frequency of 50.0 Hz and camera speed of 400 fps, for both the signal modulation produced by the LPPS itself or by means of the ED acting on the LPPS.

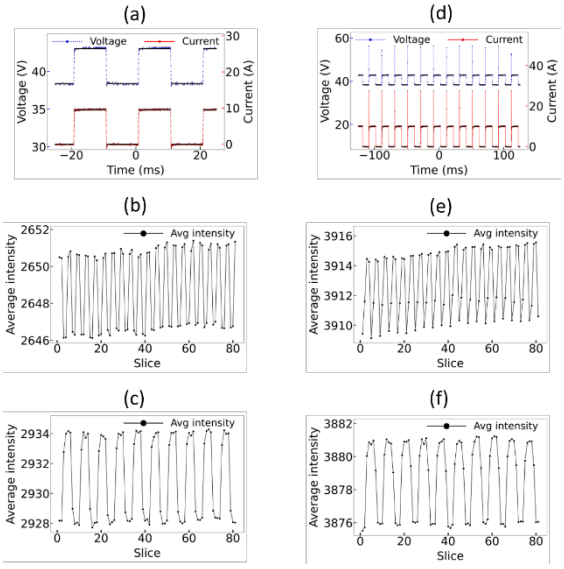

Figure 3: (a, d) Current intensities and voltages at the entrance of the inspected module, generated with the use of the LPPS by means of the power source itself (a) or by means of the ED acting on a DC signal from the LPPS (d), for ν=50.0 Hz. (b-f) Pixel intensity variations measured with the InGaAs camera vs number of captured images corresponding to (a) for camera´s velocities of 200 fps (b) and 400 fps (c), and corresponding to (d) for camera´s velocities of 200 fps (e) and 400 fps (f), respectively

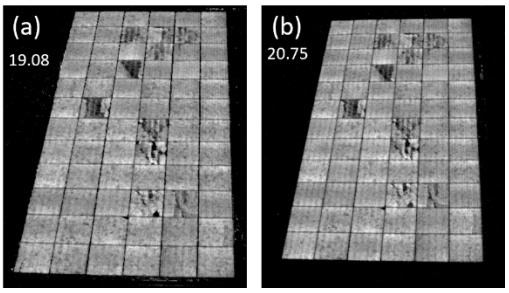

Figure 4: dEL images obtained after the post-processing of a sub-stack of 200 images, for both the signal modulation produced by the LPPS itself (a) or by means of the ED acting on a DC signal from the LPPS (b), for the case ν=50.0 Hz and camera speed of 400 fps (G=500 W/m^2 in (a), while G=840 W/m^2 in (b)). (The SNR_{25} value is indicated on the right upper part of the images)

10.4229/EUPVSEC2025/3BO.11.5
020205-003

3.3 dEL inspection of a string of 8 modules by acting on the LPPS

We have also checked the signal modulation produced by the ED for a larger number of excited modules. In particular, in this section we show the case of using the LPPS for exciting 8 modules, comparing again the signal modulation when using the LPPS itself to produce it, respect to the situation of producing the modulation by the ED acting on a DC signal from the LPPS. Figure 5 (a-c) show the current intensities and voltages measured at one module, the one which is inspected with the InGaAs camera. The square wave produced by the LPPS itself is nearly perfect (with some round corners at the beginning of the "on" and "off" periods), whereas the ED produces again transients at the beginning of the cycles. In this case, there is a double transient effect, with a first large and sharp increase in current intensity, followed by a more persistent transient of approx. 7 ms. Figure 5(d-f) shows again the pixel intensities vs the number of images measured with the InGaAs camera. It can be observed that for the case of the modulation produced by the ED acting on the LPPS, the large and sharp transient at the beginning of the cycle is not reflected on the pixel intensities, but the more persistent transient is.

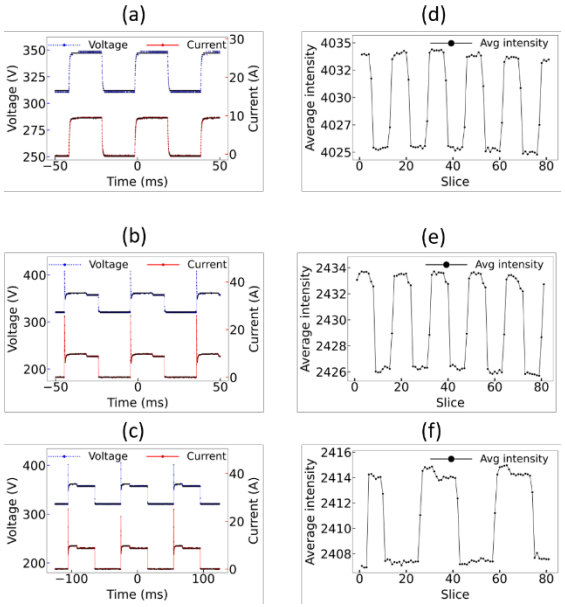

Figure 5: (a – c) Current intensities and voltages at the entrance of the inspected module (8 modules were powered in this case), for both the signal modulation produced by the LPPS itself for ν=25.0 Hz (a) or by means of the ED acting on the LPPS for ν=25.0 Hz (b) and ν=12.5 Hz (c). (d – f) Pixel intensity variations measured with the InGaAs camera vs number of captured images, for a camera velocity of 400 fps, corresponding to (a), (b) and (c), respectively

Figure 6 shows the obtained dEL images for both the signal modulation produced by the LPPS itself or by means of the ED acting on the LPPS, for ν=25.0 Hz and a camera speed of 200 fps. The quality of the dEL images are completely similar, not being affected by the transients. In any case, it is not likely very convenient the generation of these kind of transients for the power source itself. We are at present studying the way to eliminate such transients generated with the use of our ED.

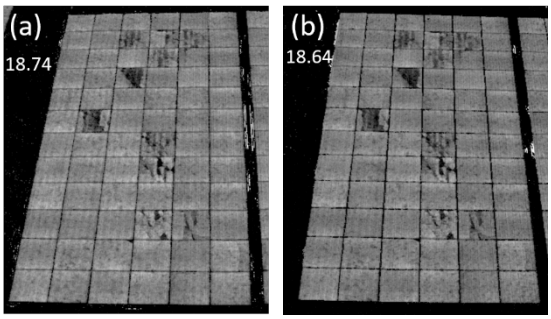

Figure 6: dEL images obtained after the post-processing of the stack of images (first 250 images), for both the signal modulation produced by the LPPS itself (a) or by means of the ED acting on the LPPS (b), for the case ν=25.0 Hz and a camera speed of 200 fps (G=840 W/m^2 in (a), while G=500 W/m^2 in (b)). (The SNR_{25} value is indicated on the right upper part of the images)

3.4 Other arrangements: dEL inspection of one module in the self-powering configuration

The advantage of the ED for signal modulation is to made it independently of the power source. In this section we show the results for the case of an individual module inspected in the self-powering configuration [15], with two other identical modules powering it. Figure 7(a, b) show the current intensities and the voltages measured at the inspected module, for frequencies of 12.5 Hz and 50.0 Hz. In this case, some sharp transients are observed both at the beginning or the end of the cycles, but not for all of them. These transients are not reflected on the pixel intensities captured by the InGaAs camera, Figure 7(c, d).

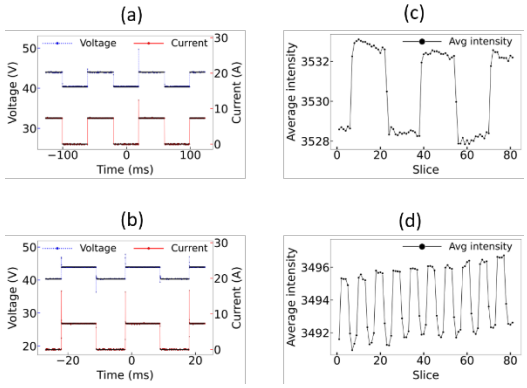

Figure 7: (a, b) Current intensities and voltages at the entrance of the inspected module, for the case of signal modulation produced by the ED acting on 2 modules (self-powering configuration), for ν=12.5 Hz (a) and ν=50.0 Hz (b). (c, d) Pixel intensity variations measured with the InGaAs camera vs number of captured images, for a camera velocity of 400 fps, corresponding to (a) and (b), respectively

Figure 8 shows the post-processed dEL images for a frequency of 12.5 Hz and a camera speed of 400 Hz, for sub-stacks of 300 and 600 images. In this case the quality is not very high due to the lower current injection (approx. 7.5 A instead of I_{sc}) into the inspected panel.

10.4229/EUPVSEC2025/3BO.11.5
020205-004

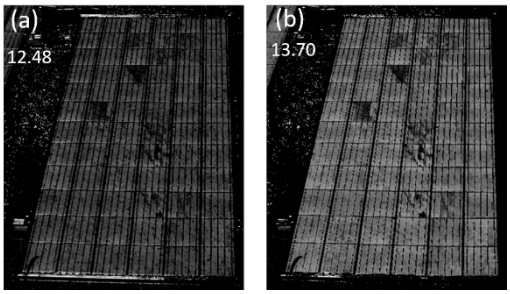

Figure 8: dEL image obtained after the post-processing of the obtained stack of images, for the case of using the ED acting on two other modules, in a self-powering configuration, for the case ν=12.5 Hz and a camera speed of 400 fps (G=840 W/m^2) (a: post-processing of the first 300 images, b: post-processing of the whole 600 images of the stack). (The SNR_{25} value is indicated on the right upper part of the images)

3.5 Analysis of the influence of frequency modulation and camera speed on image quality

We have previously shown the effect on the dEL image quality of processing sub-stacks of different number of images. In this section we will show more details of this dependence, and will analyze also the influence of the acquisition parameters (modulation frequency and camera speed) on the image quality. We have used a complete set of measurements, in particular for the case of the signal modulation produced by the LPPS itself, inspecting just one module (see section 3.2).

The previously mentioned tendency of the SNR_{25} value to decrease with the diminution of the number of processed images is shown in Figure 9, for different frequencies and camera speeds. On the other hand, it is observed that the SNR_{25} marker increases as the frequency of the modulated signal increases from 6.25 Hz to 50.0 Hz, for a camera velocity of 400 fps. Moreover, for a fixed frequency of 12.5 Hz, the SNR_{25} marker increases for a camera velocity of 200 fps respect to the case of 400 fps.

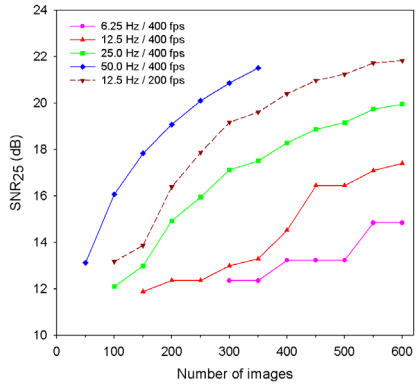

Figure 9: SNR_{25} values obtained after the post-processing of the acquired stacks of images vs number of images of the sub-stack. The data have been obtained for the case of using a programmable source with the signal generated by the power source itself. Different frequencies were used (6.25, 12.5, 25.0 and 50.0 Hz) for a camera velocity of 400 fps. For ν=12.5 Hz, two cameras velocities of 200 and 400 fps were used

This behavior is well understood when we observe the trend of the SNR_{25} marker vs the number of captured cycles for the different sets of data, Figure 10. Clearly, the SNR_{25} value depends nearly linearly with the number of cycles, varying in a minor way with the specific values of frequency and camera speed.

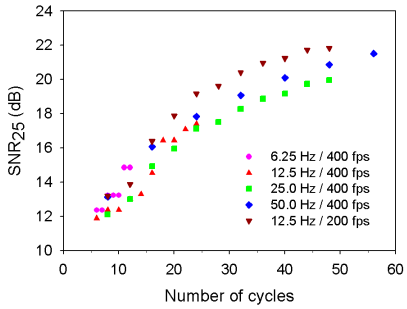

Figure 10: SNR_{25} values vs number of cycles, for the set of data of Fig. 9

We have previously observed that SNR_{25} values of around 16 are enough for a good image quality [14]. This value can be obtained, for instance, for the case of ν=50.0 Hz and a camera speed of 400 fps, for just 16 cycles (100 images), which means inspection times of 250 ms per module. Figure 11 shows, for instance, the obtained dEL images for this especific situation, for sub-stacks of 50, 100, 150 and 200 images.

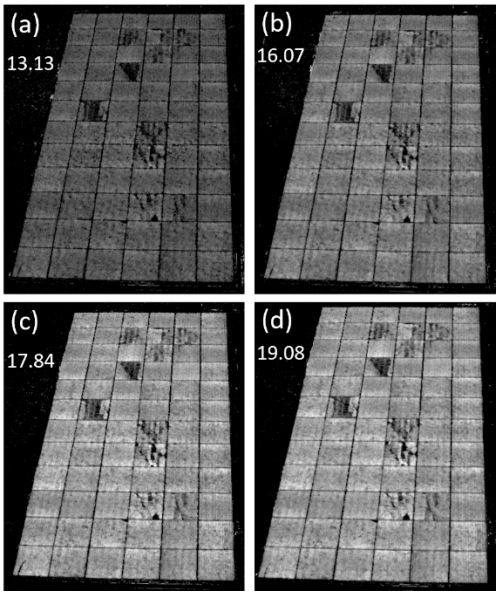

Figure 11: dEL images obtained after the post-processing of the obtained stack of images for the case of signal modulation produced by the LPPS itself, injecting current in only one panel, for the case ν=50.0 Hz and a camera speed of 400 fps (G=500 W/m^2). (a) 50 images; (b) 100 images; (c) 150 images; (d) 200 images. (The SNR_{25} value is indicated on the right upper part of the images)

Good image quality could be obtained in even shorter times when working with higher camera speeds (up to 600 fps). The combination of very short inspections times per module and the possibility to perform the modulation for every kind of power sources, even in the self-powering

10.4229/EUPVSEC2025/3BO.11.5
020205-005

configuration or in the dPL mode, has therefore the potential to provide a fast and cost-effective inspection of solar modules condition.

4 CONCLUSIONS

In this study, we present a novel approach to asynchronous daylight luminescence inspection that eliminates the need for expensive programmable power sources. This simplifies and accelerates the deployment of these powerful techniques in the field. Our compact external device successfully modulates DC signals from various sources, including small and large power sources, as well as neighboring modules, in a self-powered configuration. dPL measurements can also be obtained.

We have demonstrated that, although the external device may introduce signal transients, this does not affect the quality of the final dEL images. Thorough analysis using the SNR_{25} metric revealed that high modulation frequencies and camera speeds enable very short acquisition times of as little as 250 ms per module without compromising image quality.

This methodology offers a cost-effective and scalable solution for inspecting large-scale solar plants. By leveraging readily available — or even self-generated — power, our approach enables high-quality luminescence imaging to be used more widely. This addresses the growing need for rapid and efficient operation and maintenance in the solar PV industry. Further work is underway to eliminate the signal transients observed with our device.

5 ACKNOWLEDGMENTS

This work has been funded by the Spanish Ministry of Science and Innovation, under project PID2023-148369OB-C43, financed by MICIU/AEI /10.13039/501100011033 and FEDER/UE, and by the Regional Government of Castilla y León (Junta de Castilla y León) and by the Ministry of Science and Innovation and the European Union NextGenerationEU / PRTR under the project “Programa Complementario de Materiales Avanzados”. K. Sulca has been funded under the call for predoctoral contracts UVa 2022, co-financed by Banco Santander. C. Terrados is also grateful for the financial support received under project PDC2022-133419-I00, funded by MCIN/AEI/10.13039/ 501100011033 and NextGenerationEU/PRTR.

6 REFERENCES

[1] L. Koester, S. Lindig, A. Louwen, A. Astigarraga, G. Manzolini, D. Moser, Renew. Sustain. Energy Rev. 165 (2022) 112616.
[2] S. Gallardo-Saavedra, L. Hernández-Callejo, M.C. Alonso-García, J.D. Santos, J.I. Morales-Aragones, V. Alonso-Gómez, A.M. Moretón-Fernández, M.A. González-Rebollo, O. Martínez, Energy 205 (2020) 117930.
[3] I. Høiaas, K. Grujic, A. Gerd, I. Burud, E. Olsen, N. Belbachir, Renew. Sustain. Energy Rev. 161 (2022) 112353.
[4] O. Kunz, J. Schlipf, A. Fladung, Y.S. Khoo, K. Bedrich, T. Trupke, Z. Hameiri, Prog. Energy 4 (2022) 042014.
[5] L. Stoicescu, M. Reuter, J.H. Werner, Proceedings 29th Eur. Photovolt. Sol. Energy Conf. Exhib., (2014) 2553.
[6] J. Adams, B. Doll, C. Buerhop, T. Pickel, J. Teubner, C. Camus, C.J. Brabec, Proceedings 32nd Eur. Photovolt. Sol. Energy Conf. Exhib., (2015) 1837.
[7] S. Koch, T. Weber, C. Sobottka, A. Fladung, P. Clemens, J. Berghold, Proceedings 32nd Eur. Photovolt. Sol. Energy Conf. Exhib., (2016) 1736.
[8] G.A. dos Reis Benatto, N. Riedel, S. Thorsteinsson, P.B. Poulsen, A. Thorseth, C. Dam-Hansen, C. Mantel, S. Forchhammer, K.H.B. Frederiksen, J. Vedde, M. Petersen, H. Voss, M. Messerschmidt, H. Parikh, S. Spataru, D. Sera, Proceedings 44th IEEE Photovolt. Specialist Conf., (2017) 2682.
[9] R. Bhoopathy, O. Kunz, M. Juhl, T. Trupke, Z. Hameiri, Prog. Photovoltaics Res. Appl. 26 (2018) 69.
[10] M. Guada, A. Moretón, S. Rodríguez-Conde, L.A. Sánchez, M. Martínez, M.A. González, J. Jiménez, L. Pérez, V. Parra, O. Martínez, Energy Science & Engineering 8 (2020) 3839.
[11] L. Koester, A. Louwen, S. Lindig, G. Manzolini, D. Moser, Solar RRL 8 (2014) 2300676.
[12] M . Vuković, M.S. Wiig, G.A. dos Reis Benatto, E. Olsen, I. Burud, Prog. Energy 6 (2024) 032001.
[13] G. A. dos Reis Benatto, R. Del Prado, T. Kari, M. Bartholomäus, L. Morino, P.B. Poulsen, S.V. Spataru, Proceedings 8th World Conference on Photovoltaic Energy Conversion, (2022) 735.
[14] C. Terrados, D. González-Francés, J. Anaya, K.P. Sulca, V. Gómez-Alonso, M.A. González, O. Martínez, Proceedings 40th Eur. Photovolt. Sol. Energy Conf. Exhib. (2023) 3DO.16.5.
[15] L.A. Carpintero, M.A. González, C. Terrados, O. Martínez, D. González-Francés, K.P. Sulca, V. Alonso, Solar Energy 301 (2025) 113913.
[16] C. Terrados, D. González-Francés, K.P. Sulca, C. de Castro, M.A. González, O. Martínez, Progress in Photovoltaics (2025) doi.org/10.1002/pip.70004.